A Performance-Based Comparison of Deep-Space Navigation using Optical-Communication and Conventional Navigation Techniques: Small Body Missions

Reza Raymond Karimi*, Tomas Martin-Mur*, Sarah Elizabeth McCandless*

Abstract

Optical communications may be used in future NASA deep-space missions, resulting in much higher data transfer rates. Those optical communication links could also be used for navigation purposes. The performance of deep-space navigation for an asteroid flyby mission using ground-based optical tracking and conventional navigation techniques was investigated in this work. We present the results of variety of asteroid flyby scenarios including low phase and high phase approach angle flybys, one slow flyby in a Trojan tour mission, and also one slow flyby in a Psyche mission. In this task, four different types of observables were simulated, namely ground-based radiometric, spacecraft on-board optical, ground-based optical tracking of spacecraft (astrometry and 2-way range magnitude), and ground-based asteroid astrometry. Different combinations of these four types of observables were compared with currently in-practice ground-based radiometric/on-board optical measurements. The results showed that the ground-based optical tracking is promising and could be a potential candidate for future deep-space navigation. Precise astrometry is not possible for active comets.

Keywords: Deep Space Navigation, Optical Tracking, Orbit Determination

1. Introduction

Since the advent of space age in late 1950s, radiometric communication between ground-based stations and space probes has been the primarily technique for deep space navigation. There are three Deep Space Network (DSN) antenna complexes located at Canberra, Australia, Madrid, Spain and Goldstone, California. All the communications between DSN and in-flight spacecraft including transmitting data to the ground and receiving commands from the ground are currently performed using radio frequencies. Communications in the optical frequencies can increase the data transferring rates significantly compared to radio frequencies. NASA has demonstrated the performance of an optical communication system in the Lunar Atmosphere and Dust Environment Explorer (LADEE) mission. This mission also performed round-trip Time of Flight (TOF) measurements that exhibited the ranging capabilities of the optical system down to errors of a few cms when compared with high-precision ephemeris [1] .

In this work, we applied the ground-based optical tracking to a small body mission scenario and compared the performance of optical tracking with that of conventional navigation techniques. In optical astrometry, we compare the spacecraft and small body against the background of stars to pinpoint the plane-of-sky position in right ascension and declination. In this paper, we present the results of a variety of asteroid flyby scenarios including low-phase and high-phase approach angle flybys, one slow flyby in a Trojan tour mission, and also one slow flyby in a Psyche mission.

**Jet Propulsion Laboratory, California Institute of Technology, 4800 Oak Grove Dr., Pasadena, CA 91109.*

The current state-of-the-art deep space navigation involves using radiometric data (Doppler, range, VLBI) from the DSN combined with on-board spacecraft images of the target asteroid as the spacecraft approaches the target, referred to as Opnav. Using the combination, it is possible to target the flyby altitude with an accuracy of a few kilometers. The results in the following sections will show how the performance of a deep space asteroid flyby navigation using ground-based optical tracking is compared to the current state-of-the-art navigation technique. See [2][3][4] for more on deep-space navigation using optical-communications.

2. Ground-based Optical Tracking

Radio-frequency tracking can produce measurements of the Doppler shift of the signal's frequency, perform ranging to measure the round-trip light-time of the signal and, when the signal is received at two distant ground sites, calculate the difference in arrival time between the two to determine the plane-of-sky position of the spacecraft. At optical frequencies, coherently measuring the Doppler shift could be very challenging, but precisely measuring the round-trip light-time has been already demonstrated in a number of missions. While at Earth's orbit it is possible to use retroreflectors to bounce laser signals, at deep-space distances that approach is not sufficient, and an active system is needed on the spacecraft to track the uplink signal and transmit the necessary ranging data on an on-board generated downlink signal. In addition, it should be possible to perform astrometric measurements by imaging the return signal against the background of stars, to determine the plane-of-sky position of the spacecraft as seen by an observatory on the ground.

Unfortunately, optical tracking is going to be affected by local weather much more than radio tracking – cloud cover, fog or dust can completely preclude the transmission of optical signals.

In addition, while it should be possible to perform optical communications and ranging down to a few degrees away from the Sun direction, high-precision astrometry will require local darkness, as atmospheric sunlight – or even moonlight – scattering can easily overcome the light received from stars. These constraints can be alleviated by deploying multiple ground terminals, close enough to be within the beam width of the returned signal, but far enough to ensure that the weather is uncorrelated and that at least one of them will be able to track under adequate conditions most of the time. The most important contributor to high-precision astrometry is going to be the release of the star catalog created by ESA's Gaia mission[5]. This catalog, together with advances in observing techniques and instrumentation, could allow for nanoradian-level ground astrometry[6].

JPL is in the process of calibrating a new camera mounted on Pomona College's 1-m telescope that will be used to demonstrate the techniques and performance achievable with narrow-field ground astrometry, in that process validating the assumptions for our analysis[6]. Work is also underway to set up a high-power laser at the Optical Communication Test bed Laboratory at Table Mountain Observatory to perform ranging experiments,[7] as well as to add ranging capabilities to a prototype deep-space spacecraft optical terminal[8].

2.1 Optical Ranging

The use of optical links to perform deep-space ranging was discussed in [9] as part of an integrated optical communications system, and it was also discussed in [10] in a monograph dedicated to optical communications. By now, it has also been tested by a few missions. Deep-space optical ranging experiments have been carried out with the Mercury Laser Altimeter on MESSENGER[11][12] with the LOLA on Lunar Reconnaissance Orbiter,[13] and, as mentioned earlier, within the Lunar Laser Communications Demonstration on the Lunar

Atmosphere Dust Environment Explorer,[1] but those systems were not designed to provide operational optical tracking capabilities that could replace radio frequency tracking systems. The development of new deep-space optical terminals may allow for the design of systems for which optical ranging is not an afterthought, but a required capability.

Error budgets for deep-space optical ranging show that accuracies from a few millimeters to a few centimeters should be possible with integration times similar to those used for radio frequency ranging[14]. Optical ranging has the advantage that is not affected by charged particles in the light path – solar plasma and ionosphere – which are one of the most important error sources for radiometric tracking. For optical ranging, and with an appropriate design of the ground and flight terminals, the dominant error source should be the uncertainty and fluctuation of the tropospheric delay through the neutral atmosphere.

The measurement model for optical ranging is the same as for radio ranging, but with no ionospheric group delay and, possibly, with a different modeling of the tropospheric delay. Optical ranging should be possible with a two-way measurement, but also as a one-way measurement if high-precision atomic clocks are available at both sides of the link.

2.2 Optical Astrometry

The Gaia catalog, once it is published and it is properly tied to the International Celestial Reference Frame[15] will improve ground-based astrometry in a number of ways. It will provide positions and proper motions for stars up to the 20th magnitude, greatly densifying the set of sources that can be used to reference spacecraft measurements. The density would also facilitate the calibration of telescope distortion, or even the real-time calibration of differential tropospheric refraction. Because so many sources will be available, the field of view of the telescope can be reduced, increasing resolution and allowing for the sampling of a smaller area of the troposphere, and thus reducing the effect of atmospheric turbulence[6]. It is expected that the absolute accuracy of the catalog will be about 7 μas for star magnitudes between 3 and 12, up to a few nanoradians for a star magnitude of 20[5]. When compared with the most accurate method for radio frequency plane-of-sky tracking – delta-Differenced One-way Ranging (delta-DOR) – astrometry has the advantage of requiring only one ground station to generate measurements, allowing for more tracking opportunities. It also has the significant disadvantage of being precluded by both cloud cover and sunlight scattering; missions near Mercury or Venus are not going to be good candidates for astrometric tracking.

One of the challenges of spacecraft astrometry is that spacecraft exhibit a large proper motion against the star background. In that, they are similar to planets and other solar system bodies. Post-processing of multiple short-exposure images can be used to fit the motion of the spacecraft and obtain a more accurate position[16].

It is expected that, when using the appropriate techniques to perform ground-based astrometry, and under favorable conditions, it should be possible to perform 5-nrad spacecraft astrometry on a 1-m telescope, and 1-nrad astrometry on a 5-m telescope[6]. The measurement model that we are using in our analysis is simply the right ascension and declination of the spacecraft, as seen from the ground observatory, in the EME2000 frame. We are assuming that observers will process their images to calibrate them and provide that data to the spacecraft navigation team.

3. **Psyche Flyby Navigation**

A representative example of the results is a slow flyby at asteroid Psyche occurring on March 13, 2026 at an altitude of 50 km with V_{inf} =0.25 km/sec. To simulate the observables, a four-month arc (Nov 13, 2025 -Mar 16, 2026) was used. The simulated data include ground-based radiometric 2-way Doppler and range, on-board spacecraft optical imaging of the asteroid, ground-based optical tracking of the spacecraft and ground-based optical tracking of the small body. The simulated data were corrupted with measurement noise to mimic the real-world observables. The criteria for comparing the navigation performance yielded by each set of data are the size of the error ellipse on the B-plane and linearized-time of-flight uncertainty at the flyby time. Table 1 presents the measurement noise level used for each type of observable. The camera on-board has IFOV of 8 arcsec and resolution of 1600 pixels.

Table 1, Measurement Noise of Different Types of Observables

Type of Measurement	Measurement Noise
2-way Doppler (Radiometric)	0.1 mm/sec
2-way Range (Radiometric)	1 m
S/C astrometry (RA & DEC)	1 miliarcsec (~5 nRad)
2-way Range (optical)	5 cm
Asteroid astrometry (RA& DEC)	1,10,100,1000 miliarcsec
On-board Opnav	0.25, 0.5, 1.0 pixel (2,4,8 arcsec)

The telescope assumed for the ground-based optical tracking has a 5-m diameter and the interval between the measurements was chosen as 300 sec.

Simulation Results

The results, in general, are very dependent on the geometry of the approach asymptote to the asteroid, and how it aligns with the along-track uncertainty, which is usually the largest error on asteroid orbits. In Psyche and Odysseus examples which are slow flybys (and eventually leads to rendezvous) the approach phase angles are near 90 deg, while the low and high approach phase angle are 33.6 and 120.6, respectively. The Psyche and Odysseus flyby navigation scenarios are most affected by the asteroid along-track ephemeris uncertainty, while for the low and high phase angle cases, partially contribution of both cross-track and along-track ephemeris uncertainty plays a role in the accuracy of flyby navigation.

The criteria for comparing the performance of the ground-based optical tracking with conventional techniques are the size of the error ellipse on the B-plane and linearized time of flight uncertainty. Table 2 presents the results of three cases, 1) ground-based spacecraft optical range measurement combined with on-board Opnav, 2) ground-based spacecraft optical astrometry (RA & DEC) and range measurements combined with on-board Opnav, and 3) Radiometric (Doppler and range) measurements combined with on-board Opnav (currently in-practice the-state-of-the-art technique). The values in the parenthetical are results when on-board Opnav imaging data are added. As can be seen, when using ground-based optical tracking (of spacecraft), there are improvements in both error ellipse size and linearized-time-of-flight (LTOF) uncertainty, with LTOF uncertainty improvement more pronounced. In case of on-board Opnav imaging data combined, the error ellipse size shrinks dramatically for both radiometric and ground-based optical tracking cases (with error ellipse size more consistent with respect to each other), while LTOF of the ground-based optical tracking case shows much better improvement compared to that of radiometric, 18 sec versus 117 sec.

Table 2, Deep Space Navigation Performance Using Different Types of Observables (Psyche)

Case	Error Ellipse - semi-major axis (km)	Error Ellipse - semi-minor axis (km)	Linearized Time of Flight (LTOF) (sec)
Ground-based S/C optical 2-way Range + (on-board Opnav)	26.936 (1.806)	15.628 (1.661)	64.823 (22.012)
Ground-based S/C astrometry & 2-way Range + (on-board Opnav)	25.163 (1.723)	13.739 (1.661)	59.592 (18.074)
Radiometric (Doppler & range) + (on-board Opnav)	29.322 (1.812)	20.116 (1.700)	160.017 (117.332)

Table 3 presents the results of ground-based spacecraft optical astrometry (RA & DEC) and range measurements (case 2 of Table 2) plus ground-based asteroid (Psyche) astrometry (RA & DEC) with different levels of noise (1,10,100, and 1000 miliarcsec) combined with on-board Opnav imaging data. Ground-based Psyche astrometry helps with the improvement of the asteroid ephemeris uncertainty resulting in more accurate flyby targeting. As can be seen from Table 3, for low noise level of Psyche astrometry measurement (1 thru 10 miliarcsec), the error ellipse size and LTOF uncertainty (before combined with on-board Opnav) are very consistent with those of case 2 of Table 2 (ground-based spacecraft optical tracking combined with on-board Opnav) and as Psyche ground-based astrometry measurement noise increases (from 10 to 1000 miliarcsec), the error ellipse size and LTOF uncertainty tend to those of case 2 in Table 2 because a higher measurement noise in Psyche ground-based astrometry will not improve the asteroid's ephemeris significantly. Also, for the cases with low measurement noise of Psyche astrometry combined with on-board Opnav (case 1 and 2 in Table 3), no significant improvement in the error ellipse size and LTOF uncertainty were made. This implies that ground-based spacecraft and ground-based asteroid optical tracking (with a low measurement noise) can reduce the need for an on-board Opnav system and DSN antennas.

Table 3, Deep Space Navigation Performance Using Different Types of Observables (Psyche)

Case	Error Ellipse - semi-major axis (km)	Error Ellipse - semi-minor axis (km)	Linearized Time of Flight (LTOF) (sec)
Ground-based S/C Astrometry & 2-way Range + Ground-based Asteroid (Psyche) Astrometry (1-sigma=1 mas) + (on-board Opnav)	1.783 (1.716)	1.754 (1.649)	16.757 (14.166)

Ground-based S/C Astrometry & 2-way Range + Ground-based Asteroid (Psyche) Astrometry (1-sigma=10 mas) + (on-board Opnav)	2.039 (1.717)	1.851 (1.656)	20.257 (15.014)
Ground-based S/C Astrometry & 2-way Range + Ground-based Asteroid (Psyche) Astrometry (1-sigma=100 mas) + (on-board Opnav)	5.300 (1.722)	3.249 (1.660)	22.718 (17.851)
Ground-based S/C Astrometry & 2-way Range + Ground-based Asteroid (Psyche) Astrometry (1-sigma=1000 mas) + (on-board Opnav)	18.227 (1.723)	12.130 (1.661)	52.983 (18.072)

Figures 1 and 2 show the error ellipses with their respective linearized-time-of-flight values. Not all ellipses in Tables 2 and 3 are exhibited on the plots.

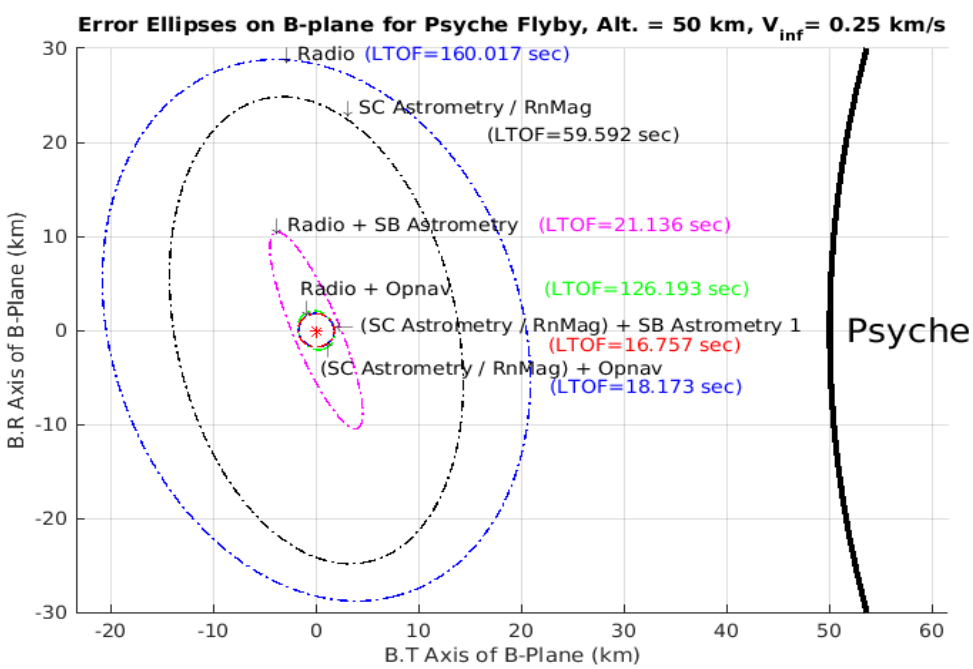

Fig.1, Error Ellipses for Psyche Flyby with Different Types of Measurements

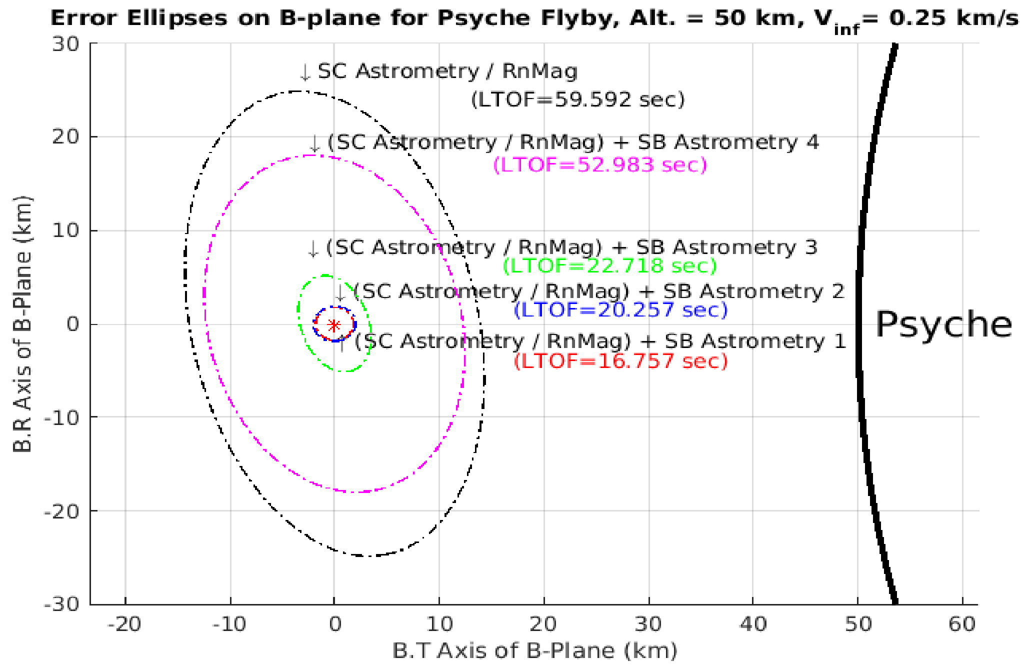

Fig.2, Error Ellipses for Psyche Flyby with S/C Astrometry / Range Mag plus Psyche Astrometry

4. Trojan Tour Flybys Navigation

A design of Trojan tour with five flybys and one final rendezvous (slow flyby here) were used to further investigate the performance of ground-based spacecraft and small body optical tracking. In this tour, we selected the rendezvous (slow flyby) asteroid , Odysseus along with two other fast asteroid flybys with high and low approach phase angles. Approach phase angles affect the on-board Opnav measurement noise, so we were interested to see how the approach phase would affect the orbit determination accuracy.

4.1 Odysseus Flyby

In our design, Odysseus flyby occurs at the altitude of 50 km at V_{inf} =0.05 km/sec on May 15, 2037. To simulate the data, a four-month arc was used spanning Jan 25, 2037 through May 08, 2037. The same measurement noise levels as Psyche (see Table 1) were used. The main difference between Psyche and Odysseus are that Odysseus is further away from sun with higher ephemeris uncertainties. Tables 4 presents the results using different types of measurements whereas Table 5 focuses on how the spacecraft orbit determination accuracy changes as Odysseus ground-based astrometry measurement noise varies. During this four-month period, Odysseus and Earth were on the same side of sun, so ground-based astrometry was possible.

Table 4, Deep Space Navigation Performance Using Different Types of Observables (Odysseus)

Case	Error Ellipse - semi-major axis (km)	Error Ellipse - semi-minor axis (km)	Linearized Time of Flight (LTOF) (sec)
Ground-based S/C astrometry & 2-way Range + (on-board Opnav)	92.804 (1.690)	29.944 (1.665)	1,013.089 (162.636)
Ground-based S/C optical 2-way Range + (on-board Opnav)	93.102 (1.692)	30.925 (1.667)	1,062.270 (288.001)
Radiometric (Doppler & range) + (on-board Opnav)	95.962 (1.739)	39.710 (1.691)	2,359.760 (850.210)

As can be seen from Table 4, the error ellipse sizes are much bigger (without on-board Opnav) than those of Psyche example mainly due to Odysseus ephemeris higher uncertainty. It's interesting to note that when on-board Opnav is included, the error ellipse size shrinks drastically, but the linearized time of flight is still high compared to the Psyche example. Table 5 shows how the results will improve using ground-based Odysseus astrometry.

Table 5, Deep Space Navigation Performance Using Different Types of Observables (Odysseus)

Case	Error Ellipse - semi-major axis (km)	Error Ellipse - semi-minor axis (km)	Linearized Time of Flight (LTOF) (sec)
Ground-based S/C Astrometry & 2-way Range + Ground-based Asteroid (Odysseus) Astrometry (1-sigma=1 mas) + (on-board Opnav)	3.637 (1.690)	2.196 (1.663)	74.740 (48.338)
Ground-based S/C Astrometry & 2-way Range + Ground-based Asteroid (Odysseus) Astrometry (1-sigma=10 mas) + (on-board Opnav)	9.516 (1.690)	2.488 (1.664)	185.223 (53.822)
Ground-based S/C Astrometry & 2-way Range + Ground-based Asteroid (Odysseus) Astrometry (1-sigma=100 mas) + (on-board Opnav)	14.884 (1.690)	7.902 (1.664)	418.225 (126.085)

Ground-based S/C Astrometry & 2-way Range + Ground-based Asteroid (Odysseus) Astrometry (1-sigma=1000 mas) + (on-board Opnav)	46.048 (1.690)	28.967 (1.665)	973.479 (162.055)

As can be seen from Table 5, ground-based Odysseus astrometry plays a significant role in estimated linearized-time-of-flight and even with on-board Opnav, although the error ellipse sizes remain small, the linearized-time-of-flight increases as Odysseus astrometry measurement noise gets higher (higher ephemeris uncertainty) . As it gets closer to the flyby date (2037), more data will be collected resulting in a more accurate ephemeris.

Figures 3 and 4 show the error ellipses with their respective linearized time of flight values. Not all ellipses in Tables 4 and 5 are exhibited on the plots.

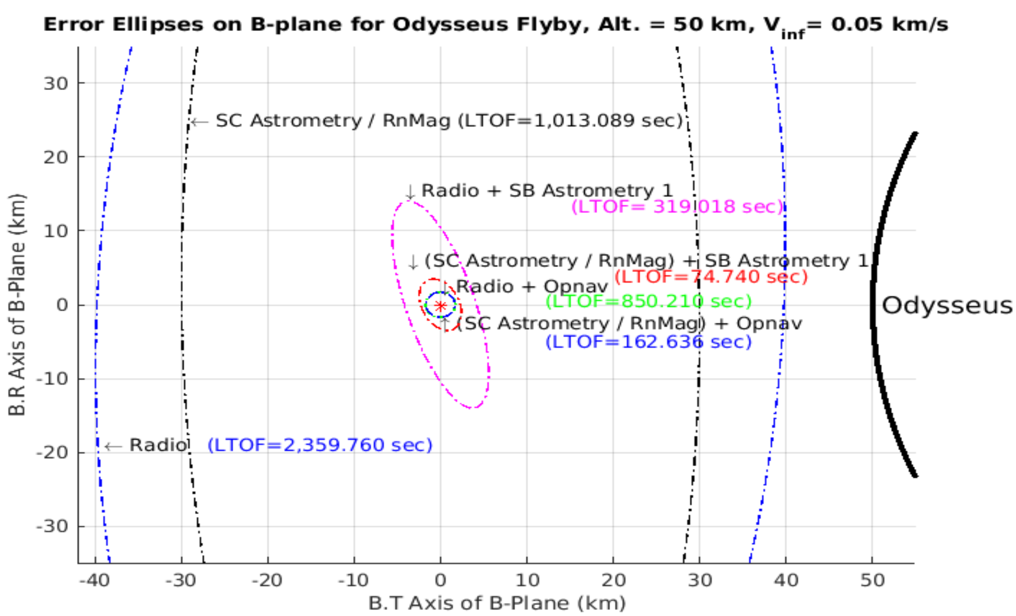

Fig.3, Error Ellipses for Odysseus Flyby with Different Types of Measurements

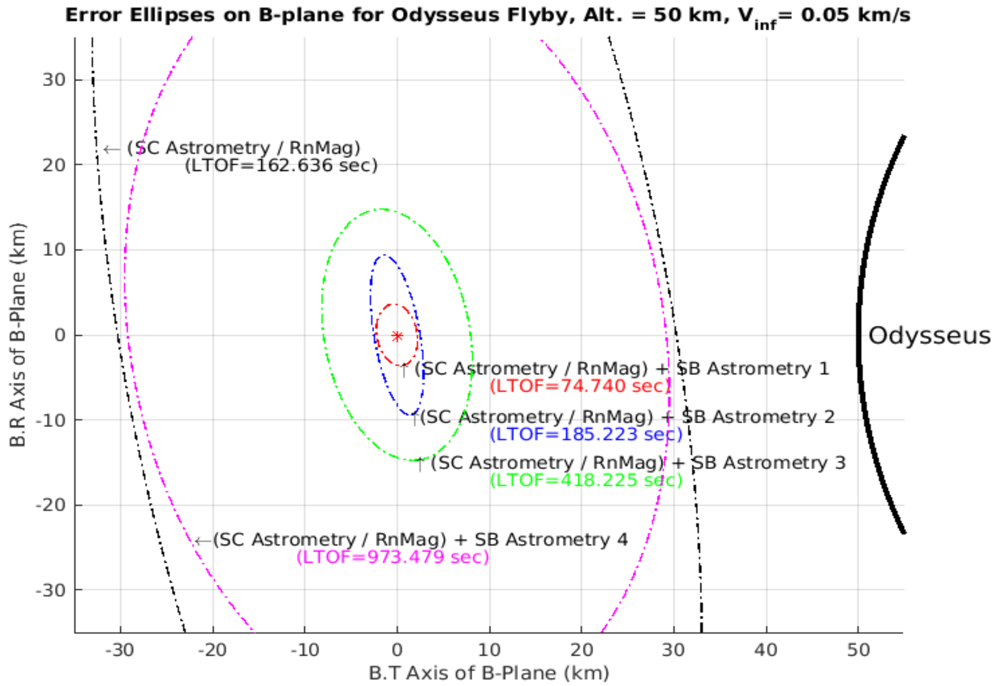

Fig.4, Error Ellipses for Psyche Flyby with S/C Astrometry / Range Mag plus Odysseus Astrometry

4.2 Pandion Flyby – 1996(TC51) - (Low Approach Phase Angle)

The asteroid Pandion 1996 (TC51) , the first in our Trojan tour design, was also used to test the performance of the deep space navigation using ground-based optical tracking. The difference between this case and the previous flyby cases are higher flyby velocity, V_{inf} =3.24 km/s, and low approach phase angle of 33.6 deg. The flyby occurs on July 20, 2032 at the altitude of 50 km. Like before, to simulated the data, a four month arc was used spanning Mar 21, 2031 thru July 13, 2032. Since the phase angle is rather small and the asteroid is more exposed to the sun light, a smaller on-board Opnav measurement noise of 0.25 pixels (~2 arcsec) was used.

Tables 6 presents the results using different types of measurements and Table 7 shows the performance of ground-based asteroid astrometry measurement for different levels of noise. Asteroid Pandion and Earth both remain on the same side of the Sun; hence, ground-based astrometry of both spacecraft and Pandion is possible.

Table 6, Deep Space Navigation Performance Using Different Types of Observables (Pandion)

Case	Error Ellipse - semi-major axis (km)	Error Ellipse - semi-minor axis (km)	Linearized Time of Flight (LTOF) (sec)
Ground-based S/C optical 2-way Range + (on-board Opnav)	300.912 (4.730)	83.959 (3.626)	58.243 (19.005)
Ground-based S/C astrometry & 2-way Range + (on-board Opnav)	300.911 (3.951)	83.897 (3.586)	58.241 (18.997)
Radiometric (Doppler & range) + (on-board Opnav)	300.915 (5.787)	84.206 (3.659)	58.251 (19.034)

Table 7, Deep Space Navigation Performance Using Different Types of Observables (Pandion)

Case	Error Ellipse - semi-major axis (km)	Error Ellipse - semi-minor axis (km)	Linearized Time of Flight (LTOF) (sec)
Ground-based S/C Astrometry & 2-way Range + Ground-based Asteroid (Pandion) Astrometry (1-sigma=1 mas) + (on-board Opnav)	2.395 (1.357)	1.947 (1.947)	0.913 (0.882)
Ground-based S/C Astrometry & 2-way Range + Ground-based Asteroid (Pandion) Astrometry (1-sigma=10 mas) + (on-board Opnav)	10.381 (3.547)	2.118 (2.109)	6.145 (1.891)
Ground-based S/C Astrometry & 2-way Range + Ground-based Asteroid (Pandion) Astrometry (1-sigma=100 mas) + (on-board Opnav)	23.635 (3.779)	5.848 (3.286)	13.964 (4.291)
Ground-based S/C Astrometry & 2-way Range + Ground-based Asteroid (Pandion) Astrometry (1-sigma=1000 mas) + (on-board Opnav)	43.819 (3.932)	40.150 (3.561)	16.729 (16.192)

As can be seen from Tables 6 and 7, the ground-based asteroid astrometry enhances the spacecraft orbit determination accuracy significantly, just compare the linearized-time-of-light of 0.913 sec (less than 1 sec) (this is the case with ground-based spacecraft and asteroid astrometry measurement using a low noise) to the linearized time of flight of 58.241 sec (this is the same case but without Pandion astrometry). When using asteroid astrometry measurements with low noise, the use of on-board Opnav becomes rather redundant.

4.3 Asteroid (2009 TM18) Flyby – (High Approach Phase Angle)

This asteroid is the last flyby object in our Trojan tour before rendezvous at Odysseus. The approach phase angle is high, 120.6 deg which makes the asteroid to be less exposed to the sun light, therefore, the on-baord Opnav measurement is noisier and we chose 1.0 pixels (~8 arcsec). The flyby occurs on June 13, 2034 at an altitude of 50 km and a velocity of V_{inf} =1.52 km/s. Like the previous cases, to simulate the observables, a four-month arc was used, spanning Feb 15, 2034 through June 06, 2034. The main difference between this case and other cases is that the asteroid and the Earth are on opposite sides of the sun; therefore, no ground-based spacecraft and asteroid astrometry is possible, and only ground-based two-way range magnitude measurement can be performed. Table 8 presents the results of orbit determination accuracy only for Radiometric, on-board Opnav, and ground-based range measurement.

Table 8, Deep Space Navigation Performance Using Different Types of Observables (2009 TM18)

Case	Error Ellipse - semi-major axis (km)	Error Ellipse - semi-minor axis (km)	Linearized Time of Flight (LTOF) (sec)
Ground-based S/C optical 2-way Range + **(on-board Opnav)**	672.186 (7.829)	87.155 (7.222)	84.284 (64.503)
Radiometric (Doppler & range) + **(on-board Opnav)**	672.189 (10.978)	88.311 (7.228)	85.799 (65.764)

In this scenario, since no ground-based asteroid astrometry is possible, the navigation has to rely merely on the on-board Opnav equipment.

Summary and Conclusion

The performance of optical communication for the purpose of asteroid mission navigation was successfully tested and compared with the performance of the-state-of-the-art techniques (ground-based radiometric and spacecraft on-board optical imaging). Asteroids with rather well-known and not very well-know ephemerides and also low and high flyby approach phase angles were used. Based on the simulated results, deep space navigation using optical communication combined with ground-based asteroid astrometry is promising and yields orbit determination accuracies at the same level of those produced by the currently in-practice techniques.

For asteroids with not very well-known ephemeris, the ground-based optical astrometry significantly improves the orbit determination accuracy; hence, the flyby linearized-time-of- flight, which is a key parameter in science data quality.

As the asteroid astrometry accuracy reduces, the delivery performance gets better and for very high asteroid astromerty measurement noise, the results tend to those of cases without ground-based asteroid astromerty.

Care has to be taken to ensure that the approach and flyby doesn't occur at low Sun-Earth-Probe (SEP) angles, as the ground-based asteroid astrometry is precluded.

Acknowledgment

We would like to thank Shyam Bhaskaran (for his advice and insightful comments), Chengxing Zhai, Michael Shao, Todd Ely, Christopher Jacobs, Joseph Lazio, and Slava Turyshev for their help with our research. This work was performed at the Jet Propulsion Laboratory, California State of Technology, under contract with the National Aeronautics and Space Administration. Government sponsorship acknowledged.

References

[1] Boroson, D. M. et al.: *Overview and Results of the Lunar Laser Communication Demonstration*, Proc. SPIE 8971, Free-Space Laser Communication and Atmospheric Propagation XXVI, 89710S (2014); doi: 10.1117/12.2045508

[2] Tomas Martin-Mur, "Spacecraft Navigation Using Optical Astrometry & Ranging," NASA SCAN Workshop on Emerging Technologies for Autonomous Space Navigation, Washington DC, February 17, 2017, https://www.nasa.gov/directorates/heo/scan/communications/navigation_workshop

[3] Tomas Martin-Mur, Sarah Elizabeth McCandless, Reza R. Karimi, "Deep-Space Navigation Using Optical Communications Systems," 26th International Symposium on Space Flight Dynamics & 31st ISTS, Matsuyama, Japan, June 3-9, 2017.

[4] Tomas Martin-Mur, Chengxing Zhai, Christopher Jacobs, Slava Turyshev, Michael Shao, Michael Peng, Sarah Elizabeth McCandless, Reza R. Karimi, "Using Optical Communications Links for Deep-Space Navigation," 2017 IEEE International Conference on Space Optical Systems and Applications, Naha, Japan, November 14-16, 2017.

[5] Prusti, T. et al.: *The Gaia Mission*, 2016, A&A, 595 A1.

[6] Zhai, C. et al.: *Nanoradian ground-based astrometry, optical navigation, and artificial reference stars*, Proc. SPIE Astronomical Telescopes and Instrumentations 2016, Ground-based and Airborne Instrumentation for Astronomy VI, Edinburgh, United Kingdom, 2016.

[7] Turyshev, S. G. et al.: *Advanced Laser Ranging and Astrometry for high-precision navigation and science investigations*, NASA Fundamental Physics Workshop, 2016.

[8] Turyshev, S. G. et al.: *Towards High-precision Navigation and Science Investigations with Deep-Space Optical Transceivers*, JPL R&TD Annual Report, R16055, 2016.

[9] Null, G. W. et al.: *Systems Analysis for Ground-Based Optical Navigation*, TDA Progress Report 42-111, 23-40, 1992.

[10] Hemmati, H. (ed.): *Deep Space Optical Communications*, JPL Deep Space Communications and Navigation Series, 50-51, 2006.

[11] Smith, D. E. et al.: *Two-Way Laser Link over Interplanetary Distance*, Science 311, 53, 2006.

[12] Cavanaugh, J. F. et al.: *The Mercury Laser Altimeter instrument for the MESSENGER mission*, Space Sci. Rev. 131, 451–480, 2007.

[13] Zuber, M. T. et al.: *The Lunar Reconnaissance Orbiter Laser Ranging Investigation*. Space Sci. Rev. 150, 63–80, 2010.

[14] Folkner, W. M. et al.: *Preliminary Error Budget for an Optical Ranging System: Range, Range Rate, and Differenced Range Observables*, TDA Progress Report 42-101, 121-135, 1990.

[15] Jacobs, C.: *Tying the Optical and Radio Celestial Reference Frames*, JPL R&TD Annual Report, R16052, 2016.

[16] Zhai, C. et al.: *Detection of a faint fast-moving near-earth asteroid using synthetic tracking technique*, Astrophyiscal Journal 792, 60–73, 2014.